

# Photoplethysmography-Based Ambulatory Heartbeat Monitoring Embedded into a Dedicated Bracelet

Simon Arberet<sup>1</sup>, Mathieu Lemay<sup>1</sup>, Philippe Renevey<sup>1</sup>, Josep Solà<sup>1</sup>,  
Olivier Grossenbacher<sup>1</sup>, Daniela Andries<sup>2</sup>, Claudio Sartori<sup>2</sup>, Mattia Bertschi<sup>1</sup>

<sup>1</sup> Swiss Center for Electronics and Microtechnology (CSEM), Neuchâtel, Switzerland

<sup>2</sup> University Hospital Center of Lausanne (CHUV), Lausanne, Switzerland

## Abstract

*Ambulatory electrocardiogram (ECG) monitors have been intensely used since half century but are still associated to clinical/ambulatory cumbersome procedures. The question of this research is the following: what is the performance of a photoplethysmography (PPG)- based device located at the wrist in terms of heart rate variability (HRV) monitoring?*

*PPG and ECG signals were recorded simultaneously on 4 subjects. Heart-beat (RR) intervals were estimated from both devices. For PPG signals, a multi-sensors approach based on the detection of local minima of the time-derivative was used to estimate RR time series. For ECG signals, an approach based on adaptive threshold was used (gold standard). The normalized differences observed on time-domain and frequency-domain HRV features were computed. Results based on 1565 minutes of recordings (N=94'000) showed an averaged correlation around 0.9 between the HRV features extracted from the PPG and ECG-based device. In view of these results, it appears that the wrist sensor opens the door towards a new generation of comfortable and easy-to-use cardiac HRV tool especially well adapted for long-term monitoring.*

## 1. Introduction

The analysis of consecutive beat intervals may provide quantitative information on the modulation of cardiac vagal and sympathetic nerve inputs and consequently constitutes one of the major clinical tool to diagnose cardiac disorders and other important diseases such as heart infarction, or severe head and brain injuries. Normal cardiac beats, labelled N, are usually identified on electrocardiograms (ECG). The NN interval series which are the time delay between two consecutive normal beats N are further analyzed in the time- or frequency-domains in order to provide non-invasive information about the autonomic nervous system [1]. Note that NN intervals consist in a sub-

group of RR intervals which includes consecutive beats R of any electrical sources (see ectopic or premature beats). Other devices based on the dry or textile electrodes principle [2] are also available but not appropriate for a continuous monitoring in daily-life situations. There is thus a lack of technologies allowing the continuous and comfortable measurement of NN intervals, to be introduced in every-day ambulatory campaigns. This study relies on the use of an alternative approach: the photoplethysmography (PPG). PPG is based on a spectrographic technology well-known in the medical community to assess arterial oxygen saturation, so-called pulse oximetry [3]. In order to monitor cardiac activity, the simplest form of PPG sensors is composed of a LED and a photo detector in contact with the skin surface [3]. At each cardiac cycle, an arterial pressure pulse propagates along the arterial tree resulting in a generalized increase of the light absorption of perfused tissues. Accordingly, cardiogenic blood volume changes modulate the absorption properties of tissues, resulting in a fluctuation of the observed PPG signal [4].

Although PPG sensors are medically accepted as a means to assess average heart rate values in pulse oximeters, little is known about the reliability of PPG signals to extract relevant HRV features [5,6]. The present validation study evaluates the performance of multi-reflectance PPG sensors integrated into a wrist device to estimate HRV features over a full night.

## 2. Method

After preparation for a full-night ECG monitoring via a digital two-lead Holter system (Lifecard CF from Space-labs Healthcare, 12-bit resolution, 10 mV dynamic range, 2.5 mV amplitude resolution, 128 samples per second), a wrist monitor integrating infrared PPG technology was placed at the left wrist of two women and two men aged between 26 and 38 years. Three PPG time series were acquired at a sampling rate of 21.33 Hz by the CSEM proprietary wrist monitor, composed of one infrared LED (940nm) and three photodiodes in contact with wrist skin.

The total weight of the device is less than 25g, and its watch-like size is 34x40x12mm.

Data was recorded during the entire night without interfering with subjects, and it was further downloaded into a PC platform. The analysis of the recorded dataset was performed offline. In a first step, reference NN intervals (and RR intervals) were extracted from raw ECGs by means of a dedicated software (Sentinel with embedded normal beat detection). In a second step, NN interval estimates were extracted from raw PPG signals using the procedure described below.

## 2.1. Heartbeat detection

First, a root mean square (RMS) signal was added to the three PPG signals, where the  $n^{th}$  sample of RMS signal  $x_4$  was computed as follows:

$$x_4(n) = \sqrt{\frac{1}{3}(x_1^2(n) + x_2^2(n) + x_3^2(n))},$$

where  $x_i(n)$  denotes the  $n^{th}$  sample of the  $i^{th}$  PPG signal. Then, cardiac beats were detected on each  $x_i$  signal independently using first derivatives  $y_i(n)$  defined as follows:

$$y_i(n) = x_i(n) - x_i(n - 1).$$

where  $y_i(n)$  is the approximation of the temporal derivate of the  $i^{th}$  PPG signal. The amplitude envelope  $\theta_i(n)$  was obtained from each derivative using a first order low-pass filter applied on the negative part  $y_i^-(n) = \min(y_i(n), 0)$  of  $y_i(n)$ :

$$\theta_i(n) = \alpha y_i^-(n) + (1 - \alpha)\theta_i(n - 1),$$

where  $\alpha = 1/32$ . The amplitude envelopes were further used to detect regions where a heartbeat could be detected, the condition for the detection being:

$$y_i(n) < \beta\theta_i(n), \quad (1)$$

where  $\beta = 2.5$  is a factor that controls the detection of the heartbeats. The value of  $\beta$  is a trade-off between false positive (small value) and false negative (large value). The position of potential heartbeats was obtained on each signal independently by searching for the minimal value in every continuous interval that fulfilled the condition given in equation (1). As the precision of the heartbeat positions is linked to the sampling period, which is relatively low, a second-order polynomial interpolation was used around the detected minimal value to increase its precision. Accordingly, an estimate of a fractional part of the sampling period that corresponded to the position of the minima was obtained. Assuming  $y_i(n_{min})$  to be a detected local minimum, the fractional part of the sampling period was estimated as:

$$n_{frac} = \frac{y_i(n_{min} - 1) - y_i(n_{min} + 1)}{2(y_i(n_{min} + 1) - 2y_i(n_{min}) + y_i(n_{min} - 1))}. \quad (2)$$

The position of the heartbeats was thus given by  $n_{min} + n_{frac}$  from each PPG signals. The final heartbeat location estimates  $\hat{R}$ , were obtained by a procedure which merges the detected heartbeats from each PPG signals ( $x_1, x_2, \dots, x_4$ ) such that the local variation of the  $\widehat{RR}$  intervals is minimized. Finally, the  $\widehat{RR}$  serie was calculated as the difference between consecutive positions of detected heartbeats  $\hat{R}$ . Figure 1 displays typical detection of R-wave peaks (cardiac muscle contractions) on ECG, the respective heartbeats detected on PPG signals and both resulting RR and  $\widehat{RR}$  series.

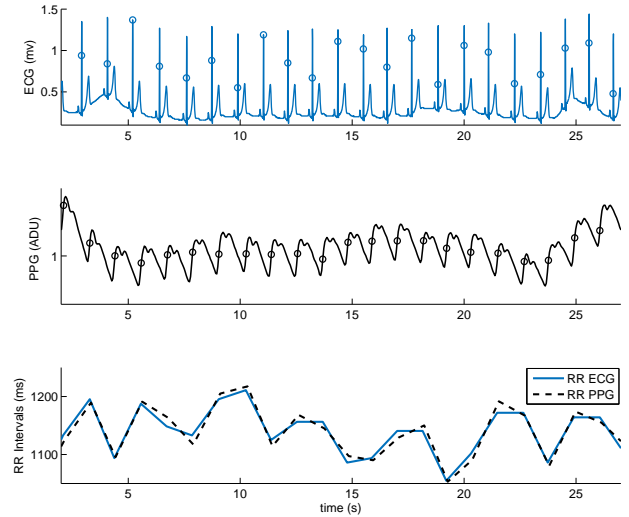


Figure 1. Illustration of typical R-wave peak detection (cardiac muscle contractions) on ECG, the respective heartbeats detected on PPG signals and both resulting RR and  $\widehat{RR}$  series.

## 2.2. Motion artefacts

In order to detect and correct the episodes which contain important motion artefacts, an approach similar to the heartbeat detection was applied to the computed  $y_i$  signals. The beginning of episodes with important artefacts was identified as the location where  $|y_i| > \alpha$  with  $\alpha$  fixed at 70. When important artefacts were locally detected on more than one PPG signal, the 10-second time interval following the detection point was not considered. An interpolation algorithm in the R domain was then applied to obtain  $\widehat{RR}$  with the lowest variation value.

### 2.3. Sequence alignment

The estimated  $\hat{R}$  (extracted from PPG signals) were converted into  $\widehat{RR}$  series. The obtained heartbeat interval or RR serie was aligned with the RR serie extracted from ECG signal (provided by the Sentinel software), via an ad-hoc proprietary algorithm in order to compensate for the difference between the time bases (offset and clock drifts) of the two measuring devices. This algorithm synchronises the two sequences every five minutes by estimating the relative delay between them via the peak detection of a correlation function.

### 2.4. Outlier rejection

To avoid that the comparison between the two heartbeat interval series be biased by ectopic, premature beats or outliers, a simple rejection procedure was applied to the series of  $\widehat{RR}$ . Any  $\hat{R}$ s associated with intervals below or above threshold values ( $< 600$  ms or  $> 1500$  ms) were removed from the series.

At the end of this procedure, uniformly sampled NN series of reference and their estimation labeled  $\widehat{NN}$  were obtained by interpolating samples at a fixed sampling rate of 4 Hz as described in the HRV guidelines [7].

### 2.5. Feature extraction

The gold standard HRV features were then computed from the resulting four uniformly resampled NN signals. These HRV features estimated over each 5-minute segments (short-term HRV analysis) are described in the following section. In the time domain, the simplest variable to calculate is the standard deviation of the NN intervals, labeled SDNN. The standard deviation of differences between adjacent NN intervals, labeled SDSD was also computed over each 5-minute segment. The units of both features are in milliseconds (ms).

Concerning the frequency domain, various methods to estimate the power spectral density exist. In this study, we relied on the Yule-Walker algorithm to estimate parametric spectral densities by fitting autoregressive (AR) prediction models of a given order to RR and  $\widehat{RR}$  series. An AR model with order 44 was fitted on each 5-minute segments used to evaluate the power in different ranges; the power in the very low frequency range, labeled VLF ( $< 0.04$  Hz), the power in the low frequency range, labeled LF ( $0.04 - 0.15$  Hz), and the power in the high frequency range, labeled HF ( $> 0.15$  Hz) [7]. The LF/HF ratio values were also computed. This last feature is often used to monitor the sympatho-vagal balance. The series of time- and frequency-domain features evaluated from synchronized ECG and PPG signals were then compared in

terms of normalized correlation, as well as the mean  $\mu$  and standard deviation  $sd$  of there difference  $\mu \pm sd$ .

## 3. Results

In this section are presented results to assess agreement between the reference Holter system and the proposed PPG system for HRV feature extraction. In total, 1565 minutes of data were analyzed, containing approximately 94'000 heartbeats.

The correlation between the temporal and frequency features of the ECG and PPG systems, of the four subjects estimated from both devices are depicted in table 1. The plots of the temporal and frequency features of one of the subjects are shown in Figures 2 and 3, respectively.

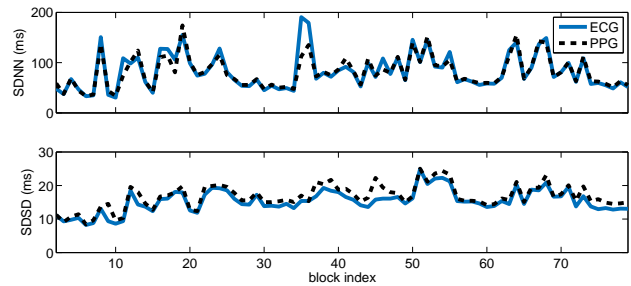


Figure 2. HRV temporal features (SDNN and SDSD) extracted from one of the subject of the database (#4). The correlation values are 0.93 and 0.95, respectively.

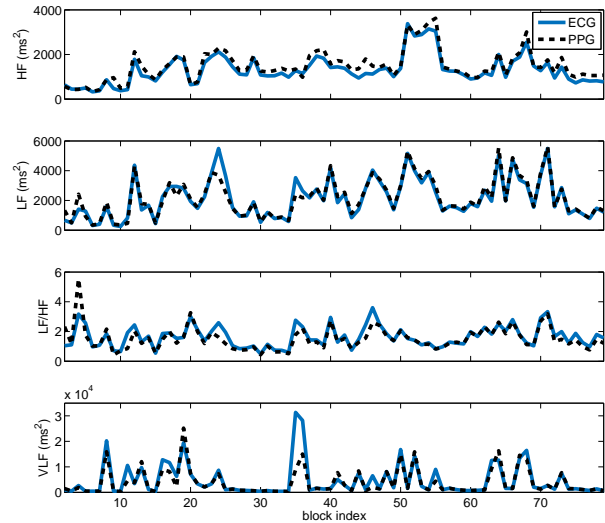


Figure 3. HRV frequency features (HF, LF, LF/HF and VLF) extracted from one of the subject of the database (#4). The correlation values are 0.98, 0.96, 0.84 and 0.86, respectively.

Results show that the two methods lead to high corre-

Table 1. The correlations values and normalized errors between the HRV features extracted from the ECG and PPG signals are displayed. The correlation is around 0.9 for all HRV features, which shows statistical agreement between both ECG- and PPG-based approaches.

Features	Temporal features		Frequency features			
	SDNN	SDSD	HF	LF	VLF	LF/HF
# 1	0.82 / 0.23	0.82 / 0.22	0.90 / 0.30	0.91 / 0.23	0.69 / 0.59	0.78 / 0.40
# 2	0.96 / 0.12	0.87 / 0.14	0.86 / 0.29	0.93 / 0.22	0.93 / 0.29	0.85 / 0.31
# 3	0.99 / 0.07	0.87 / 0.18	0.88 / 0.32	0.98 / 0.14	0.96 / 0.23	0.85 / 0.25
# 4	0.93 / 0.15	0.95 / 0.11	0.98 / 0.16	0.96 / 0.14	0.86 / 0.43	0.84 / 0.25
Average correlation	$0.93 \pm 0.06$	$0.88 \pm 0.05$	$0.91 \pm 0.04$	$0.95 \pm 0.03$	$0.86 \pm 0.11$	$0.83 \pm 0.03$
Average normalized error	$0.14 \pm 0.06$	$0.16 \pm 0.04$	$0.27 \pm 0.06$	$0.18 \pm 0.04$	$0.39 \pm 0.14$	$0.30 \pm 0.06$

lated values for all the temporal and frequency features. The average correlation is around 0.9 on all features. The most correlated features being the SDNN, HF and LF which have an average correlation of respectively  $0.93 \pm 0.06$ ,  $0.91 \pm 0.04$  and  $0.95 \pm 0.03$ , while the worst correlation, on the LF/HF feature, is still above 0.8 ( $0.83 \pm 0.03$ ).

As can be observed in Figures 2 and 3, the difference between the HRV features extracted from the PPG and ECG is mostly due to errors in few segments, which also explained why the relative error shown in table 1 can be relatively high even if the signals are highly correlated. A deeper investigation on the raw PPG signals shows that these errors are due to strong motion artefacts that leads to very strong noise in the PPG signal. Moreover these artefacts are very difficult to correct due to the absence of relevant information on a large temporal interval. As these motion artefacts are identified (see section 2.2), it is possible to discard them if we want to only keep the segments where a very accurate HRV value is desired.

#### 4. Conclusion

We presented a study that demonstrates based on the long-term recording of four healthy subjects, that the HRV features computed from  $\widehat{RR}$  intervals estimated via the analysis of PPG signals recorded at the wrist level are in agreement with simultaneous HRV features computed from RR intervals measured by from ECG signals. A correlation of around 0.9 has been shown for both temporal and spectral HRV features. The use of comfortable sensors such as the suggested wrist device might in the future provide novel insights into cardiovascular regulation mechanism occurring during sleep.

#### Acknowledgements

This study was made possible by grants from the Wilsdorf Foundation. The authors would like to thanks the collaborators of CHUV responsible for the data acquisition.

The authors would also like to thanks all CSEM's collaborators who were involved in the design and development of the wrist-located PPG device.

#### References

- [1] Sztajzel J, et al. Heart rate variability: a noninvasive electrocardiographic method to measure the autonomic nervous system. *Swiss medical weekly* 2004;134:514–522.
- [2] Webster JG. *The Measurement, Instrumentation, and Sensors: Handbook*. Springer Verlag, 1999.
- [3] Webster JG. *Design of pulse oximeters*. Taylor & Francis, 2002.
- [4] Higgins JL, Fronck A. Photoplethysmographic evaluation of the relationship between skin reflectance and skin blood volume. *Journal of biomedical engineering* 1986;8(2):130–136.
- [5] Shelley KH. Photoplethysmography: beyond the calculation of arterial oxygen saturation and heart rate. *Anesthesia and analgesia* 2007;105:S31–S36.
- [6] Dehkordi P, et al. Pulse rate variability compared with heart rate variability in children with and without sleep disordered breathing. In *35th Annual International Conference of the IEEE Engineering in Medicine and Biology Society*. Osaka, 2013; 6563–6566.
- [7] Malik M. Heart rate variability. standards of measurement, physiological interpretation, and clinical use. *Circulation* 1996;93:1043–1065.

Address for correspondence:

Dr. Simon Arberet  
 CSEM SA  
 Jacquet-Droz 1  
 CH-2002 Neuchâtel  
 Switzerland  
 simon.arberet@csem.ch